Ion irradiation of epitaxial $YBa_2Cu_3O_{7-\delta}$ films: Effects of electronic energy loss

B. Hensel, B. Roas,* S. Henke, R. Hopfengärtner, M. Lippert, J. P. Ströbel, M. Vildić, and G. Saemann-Ischenko
Physikalisches Institut, Universität Erlangen, Erwin-Rommel-Strasse 1, D-8520 Erlangen, Federal Republic of Germany

S. Klaumünzer
Hahn-Meitner-Institut, Bereich Schwerionenphysik, Glienicker Strasse 100, D-1000 Berlin 39, Federal Republic of Germany
(Received 27 February 1990)

We have performed MeV-ion irradiation of high-quality epitaxial $YBa_2Cu_3O_{7-\delta}$ films (thickness ≈ 200 nm) at low temperatures (60 to 80 K) with *in situ* measurements of the resistivity ρ and the critical temperature T_{c0}. The increase of ρ and the decrease of T_{c0} observed for irradiation with 6-MeV ^{4}He and 25-MeV ^{16}O are proportional to the calculated number of atoms displaced by processes of the *nuclear* energy loss S_n. For 25-MeV ^{32}S, 120-MeV ^{86}Kr, 173-MeV, and 360-MeV ^{129}Xe, however, a much stronger sensitivity to irradiation is observed than would be expected from these calculations. Furthermore, ρ and T_{c0} depend nonlinearly on ion fluences in the cases of 173- and 360-MeV ^{129}Xe. The enhanced sensitivity to irradiation and the deviations from linearity are attributed to effects of additional defects induced by the *electronic* energy loss S_e. If S_e exceeds an effective threshold S_{e0} of 2000 eV/Å, latent tracks of amorphized material are observed. A model is proposed that qualitatively describes the effects of these tracks on transport properties.

I. INTRODUCTION

Since highly oriented thin films or slices of dense polycrystalline bulk material of high-T_c superconductors have been available, numerous ion-irradiation experiments have been performed,[1-13] mainly with $YBa_2Cu_3O_{7-\delta}$ (Y-Ba-Cu-O). The projectiles and energies used in these experiments ranged from ^{1}H to ^{129}Xe and from less than 1 MeV to several GeV. The main concern of all these investigations has been the interpretation of effects of irradiation-induced lattice defects on superconductivity and normal-state properties of the copper-oxide-based high-T_c compounds.

For most combinations of ion species and energies, two mechanisms of interaction between the incident ions and the crystal lattice are dominant, commonly termed *nuclear* energy loss S_n and *electronic* energy loss S_e. Only in the case of ions with kinetic energies far above the Coulomb barrier may the decay products of nuclear reactions also be important for defect production.[5] The nuclear energy loss S_n results from energy transfer from projectiles to target atoms in elastic collisions, (i.e., without excitation of internal degrees of freedom) while S_e originates from ionization and/or electronic excitations of target atoms. S_n leads to defect production for all kinds of ions, projectile energies, and target materials provided the transferred energy lies above a material-dependent displacement threshold T_d. In contrast, defect production via electronic excitations and/or ionizations requires an additional mechanism to convert excitation energy into atomic motion. In fact, on the one hand, there are materials (e.g., halides, polymers), the structure of which is quite sensitive to electronic excitations. On the other hand, there are materials (e.g., β-alumina, crystalline Si), the structure of which is stable against electronic excitations even at the highest S_e values experimentally accessible. Numerous materials (e.g., vitreous silica,[14] silicate minerals, iron garnets,[15,16] metallic glasses,[17] pure gallium,[18] and iron[19]) are between these two extreme cases, i.e., there exists an effective electronic energy-loss threshold S_{e0}, below which defect production is predominantly due to S_n and above which the structure becomes progressively sensitive to electronic excitations. Consequently, whether, in a given material, S_e contributes to defect production cannot be judged definitely by experiments using ions with low or moderate electronic energy loss but one has to use fast heavy ions with kinetic energies in the range of several MeV/amu.

The results of the experiments of this work definitely confirm those of previous work,[10] namely that the *electronic* energy loss S_e considerably contributes to the irradiation damage in the high-T_c compound Y-Ba-Cu-O. This judgment results from data obtained in a variety of irradiation experiments with a large number (>50) of nearly identical and well-characterized samples, with the relevant parameters S_n and S_e spanning several orders of magnitude. We will also propose a model for the anomalous irradiation effects observed for 173- and 360-MeV ^{129}Xe.

II. SAMPLES AND EXPERIMENT

All samples have been prepared by laser ablation in an *in situ* process onto (100) $SrTiO_3$ substrates at Siemens AG, Erlangen. The preparation process is described in full detail in Ref. 20. In this context it should be emphasized that almost all properties of these epitaxial films were obtained in a highly reproducible manner. A

variety of experiments have been performed with nearly identical samples, establishing a good knowledge of the properties of the undamaged material. The results of x-ray-diffraction analysis, high-resolution transmission electron microscopy (HRTEM), and Rutherford backscattering, together with the data of the resistivity $\rho(T)$, Hall coefficient $R_H(T)$,[21] critical current $j_c(\mathbf{B},T)$,[22] and of dynamic properties, such as far-infrared reflectivity[23] and high-frequency conductivity,[24,25] as well as results obtained by conversion-electron Mössbauer spectroscopy[26] underline the high quality of the samples used in our experiments. In this paper, however, we shall address only the basic properties $\rho(T)$ and T_{c0}.

Before irradiation, the state of the films is characterized by a resistivity $\rho(100\ \text{K}) \approx 100\ \mu\Omega\ \text{cm}$, a critical temperature $T_{c0}(\rho=0)$ between 86 and 91 K, transition widths $\delta T_c \leq 1$ K, and a resistivity ratio $\rho(300\ \text{K})/\rho(100\ \text{K})$ of about three (with linear temperature dependence in between). The thicknesses of the films ranged from 100 to 300 nm. To allow four probe measurements they were patterned by photoresist and wet etching (without degradation of sample properties) to striplines of 50-μm width and 1.7-mm length or 10-μm width and 180-μm length.

The ion irradiations were performed at the low-temperature irradiation facilities of the Erlangen tandem Van de Graaff accelerator and of Vicksi at the Hahn-Meitner Institut, Berlin. Table I lists the projectiles and energies selected for our experiments, together with the calculated values of S_n, S_e, and of the projected ranges in Y-Ba-Cu-O. Since the ranges of the used projectiles exceed 5 μm, which is much more than the specimen thickness, implantation is completely negligible. The energy losses S_n and S_e spanned a wide range to clearly separate the different effects of the two underlying damage mechanisms. During irradiation, electromagnetic beam sweeping was used to ensure homogeneous irradiation conditions. Consequently, no undesired effects, like extensively broadened or split phase transitions, were observed.

Computerized measurements of $\rho(T)$ were performed *in situ* after each irradiation fluence, i.e., without heating the samples to more than 120 K. The sample temperature was determined by a platinum resistor with a relative accuracy of about 0.1 K. The sample resistance was measured with current inversion, resulting in an error of $<0.1\%$. The current density for these measurements was about 100–500 A/cm^2 and no effect on $\rho(T)$ or T_{c0} was observed even for the highest applied currents. T_{c0} was determined as the highest temperature T where the condition $\rho(T)=0$ is fulfilled within experimental accuracy. During irradiation the cryostat temperature T_{irr} was held constant in the range between 60 and 80 K. The sample temperature was not significantly raised during irradiation, as can be concluded from the observation that the samples remain superconducting (of course, this is only true if $T_{c0} > T_{\text{irr}}$).

III. RESULTS AND DISCUSSION

In the following sections the changes of the resistivity $\rho(100\ \text{K})$ and the critical temperature T_{c0} due to an ion fluence Φ will be given as normalized quantities $\Delta\rho$ and ΔT_{c0}:

$$\Delta\rho = \frac{\rho(\Phi, T=100\ \text{K}) - \rho(\Phi=0, T=100\ \text{K})}{\rho(\Phi=0, T=100\ \text{K})} ,$$

$$\Delta T_{c0} = \frac{T_{c0}(\Phi) - T_{c0}(\Phi=0)}{T_{c0}(\Phi=0)} .$$

TABLE I. Calculated projected ranges and energy losses S_n and S_e in Y-Ba-Cu-O for the given projectiles and energies [computer code PRAL (Ref. 27)].

Projectile	Energy (MeV)	Range (μm)	S_n (eV/Å)	S_e (eV/Å)
^{4}He	6	16	0.02	25
^{16}O	25	9	0.25	250
^{32}S	25	5	1.7	710
^{86}Kr	120	11	5.3	1800
^{129}Xe	173	9	11	2400
^{129}Xe	360	16	6.2	2800

Figure 1 exemplarily shows a set of $\rho(T)$ curves for several fluences of 25-MeV ^{16}O [Fig. 1(a)] and 360-MeV ^{129}Xe [Fig. 1(b)], with the resistivity normalized to its

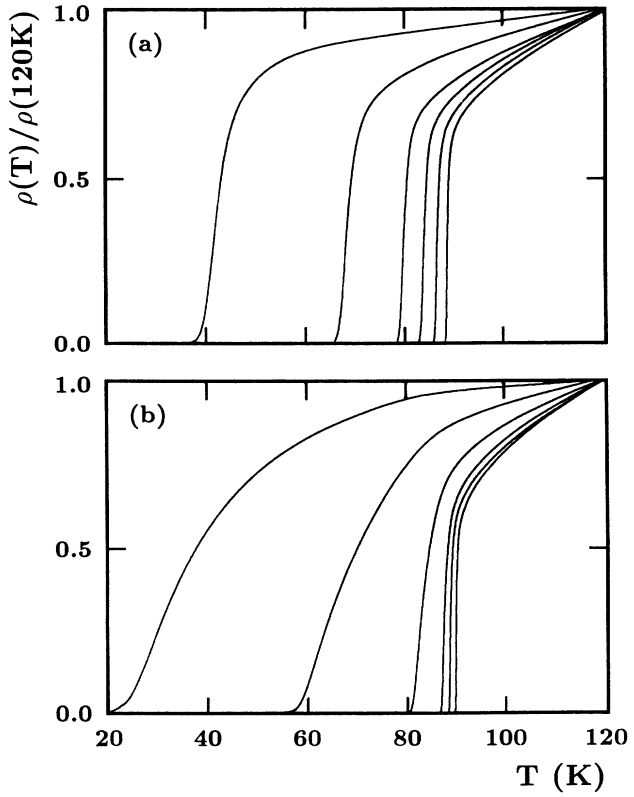

FIG. 1. Plot of $\rho(T)/\rho(120\ \text{K})$ for (a) 25-MeV ^{16}O fluences of 0, 2, 5, 10, 20, and 40×10^{14} cm^{-2} and (b) 360-MeV ^{129}Xe fluences of 0, 2, 5, 10, 20, and 30×10^{11} cm^{-2}.

TABLE II. Total displacement cross section P due to the nuclear energy loss S_n in Y-Ba-Cu-O for the given projectiles and energies [computer code TRIM (Ref. 27) with a displacement energy of 20 eV and complete cascade calculation].

Projectile	Energy (MeV)	S_n (eV/Å)	P (cm^2)
^4He	6	0.02	2.86×10^{-19}
^{16}O	25	0.25	5.56×10^{-18}
^{32}S	25	1.7	3.33×10^{-17}
^{86}Kr	120	5.3	9.10×10^{-17}
^{129}Xe	173	11	1.41×10^{-16}
^{129}Xe	360	6.2	1.00×10^{-16}

value at 120 K. Note that in both cases a metallic behavior of $\rho(T)$ is still observed after irradiation, in spite of the drastic reduction of the critical temperature. No semiconducting behavior of the resistivity is observed unless $T_{c0}<10$ K. A closer look at the two plots, however, suggests that some differences in the damage mechanisms of the two projectiles must exist. While the phase transitions remain relatively narrow for 25-MeV ^{16}O even at high fluences, a severe broadening with only a slight shift of the onset to superconductivity is observed for 360-MeV ^{129}Xe. This finding is in agreement with results obtained for bulk material irradiated with 3.5-GeV Xe ions.[10] Another indication for different mechanisms is the fact that the resistivity increases nonlinearly with fluence for 173- and 360-MeV ^{129}Xe (Fig. 2), in contrast to a linearity between $\Delta\rho$ and Φ observed for 25-MeV ^{16}O (Fig. 3) and 6-MeV ^4He. Calculations of the total cross section P of displacements via S_n (Table II) using the computer code TRIM (Ref. 27) allow a "reduction" of the ion fluences to the projectile-independent quantity DPA $P\Phi$ (DPA = displacements per atom). Doing so for 6-MeV ^4He and 25-MeV ^{16}O Fig. 3 is obtained. Within experimental accuracy no significant differences between the two projectiles are observed, indicating that the same underlying mechanism should be dominant in both cases, namely S_n.

A plot of the fluence dependences of $\Delta\rho$ for all projectiles is depicted in Fig. 4, while the dependences on the number of displaced atoms are shown in Fig. 5. It is obvious that a mechanism of radiation damage other than the mere energy loss in elastic collisions dominates the resistivity increase for high-energy ^{86}Kr and ^{129}Xe. Even for ^{32}S we observe apparent deviations from the "scaling behavior" which is observed for the lighter projectiles. The same trend is found for the corresponding data of the decrease of the critical temperature T_{c0} (Figs. 6 and 7), although the experimental errors in the determination of T_{c0} result in slightly scattered data.

A better test of the assumption of different mechanisms of irradiation damage and its effects on electronic transport and superconductivity is the plot of the resistivity increase $\Delta\rho$ versus the decrease of the critical tempera-

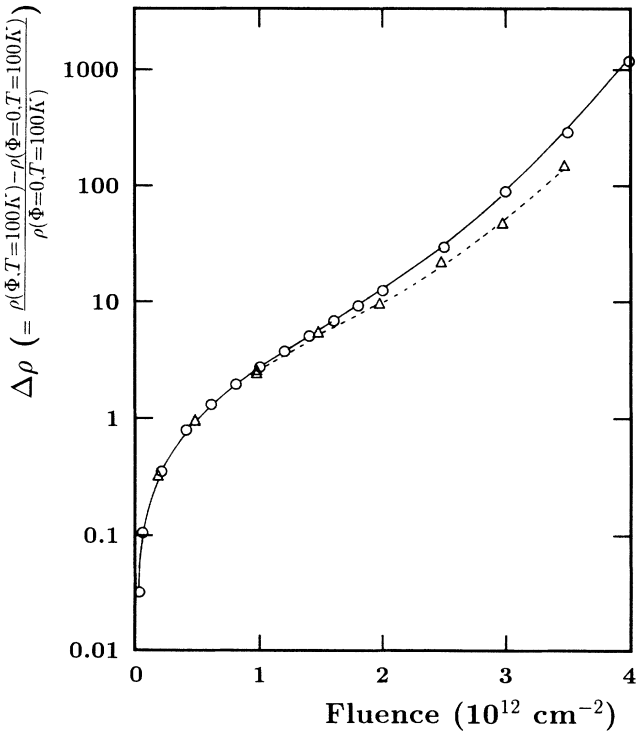

FIG. 2. Variation of $\Delta\rho$ for irradiation with 360-MeV ^{129}Xe at 100 K (circles) and 173-MeV ^{129}Xe at 80 K (triangles).

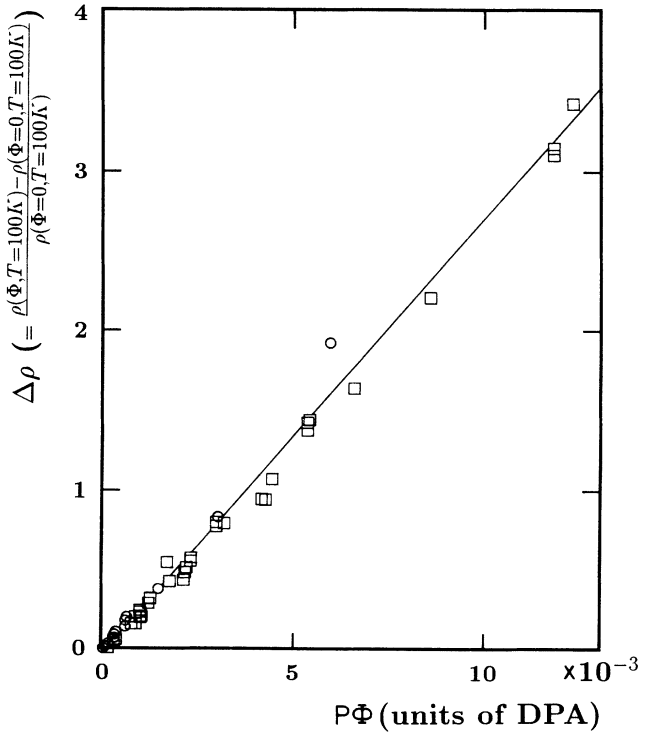

FIG. 3. Plot of $\Delta\rho$ vs $P\Phi$ in units of DPA, where DPA = displacements per atom, for 6-MeV ^4He (circles) and 25-MeV ^{16}O (squares).

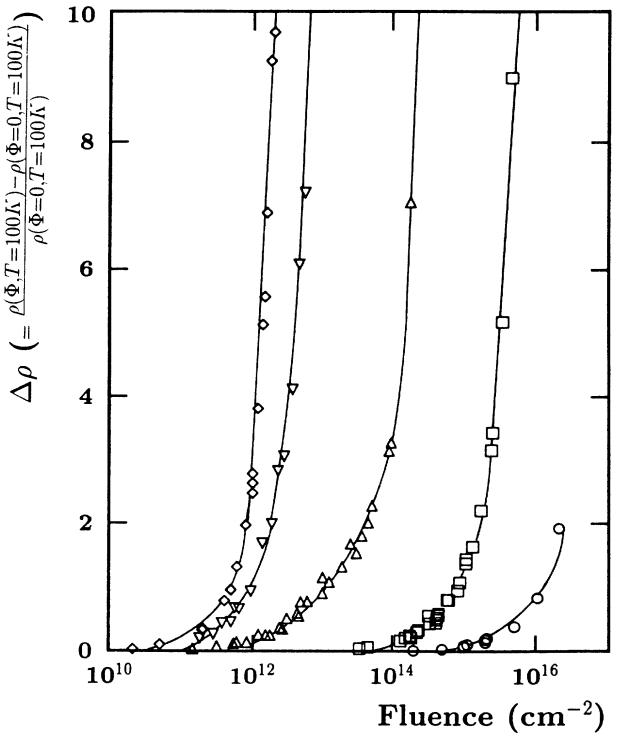

FIG. 4. $\Delta\rho$ against fluence for 6-MeV ^{4}He (circles), 25-MeV ^{16}O (squares), 25-MeV ^{32}S (triangles), 120-MeV ^{86}Kr (inverted triangles), 173- and 360-MeV ^{129}Xe (diamonds).

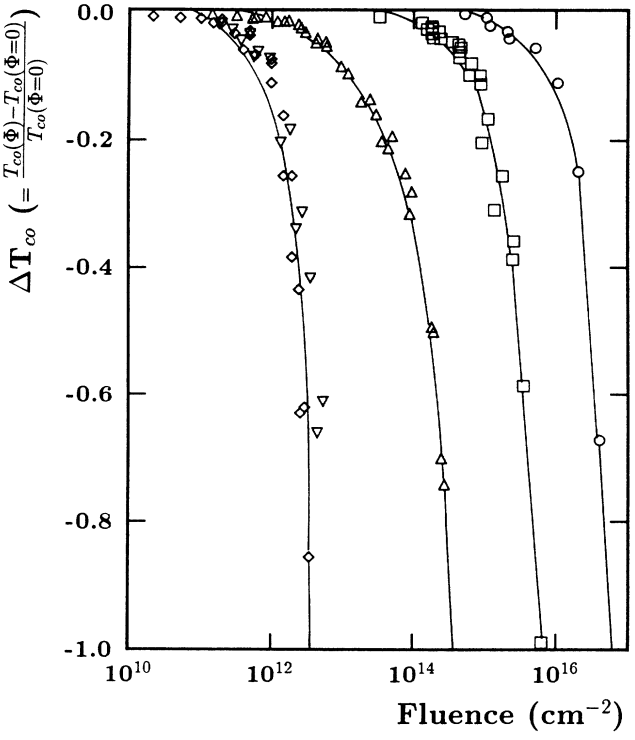

FIG. 6. ΔT_{c0} against fluence for all projectiles (for symbols see Fig. 4).

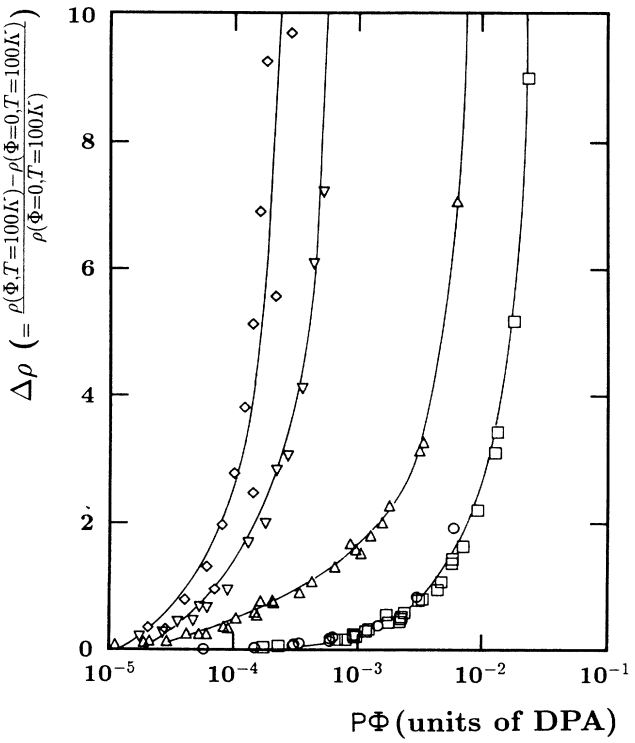

FIG. 5. Variation of $\Delta\rho$ with $P\Phi$ (units of DPA) for all projectiles (symbols as in Fig. 4).

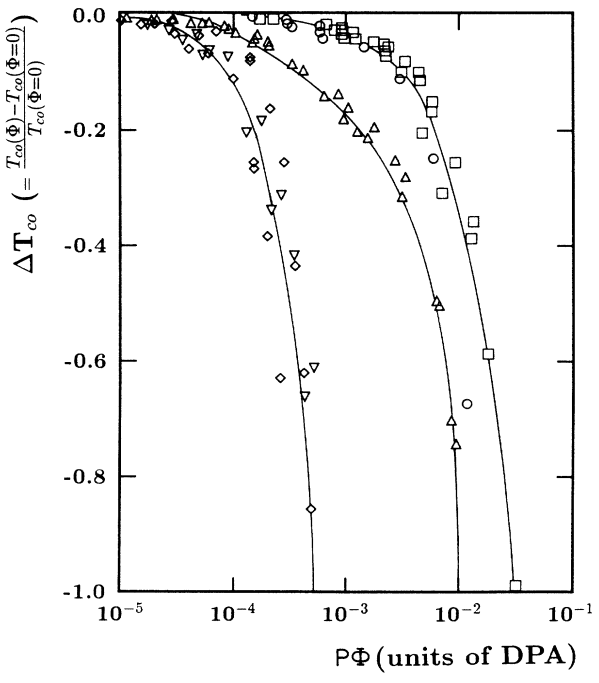

FIG. 7. Variation of ΔT_{c0} with $P\Phi$ (units of DPA) for all projectiles (for symbols see Fig. 4).

ture ΔT_{c0} (Figs. 8 and 9). This plot avoids both the numerical uncertainties of DPA calculations due to unknown displacement thresholds as well as the dubiousness of their physical relevance to characterize the defect concentration, e.g., due to the neglect of defect recombination. It is evident from Fig. 9 that the data for 173- and 360-MeV ^{129}Xe differ significantly from the uniform behavior of all other projectiles (Fig. 8).

A closer analysis showed that differences in the energy spectra of the primary recoils induced via elastic collisions cannot account for this nonscaling. Hence, it is suggestive to ascribe this nonscaling to an additional damage mechanism which originates from electronic excitations and/or ionizations of target atoms. Although the electronic energy loss varies from 25 to 1800 eV/Å (Table II) going from 6-MeV ^{4}He to 120-MeV ^{86}Kr the $\Delta\rho$-ΔT_{c0} data of these ions scale nicely (Fig. 8). Obviously, S_e has to surmount a certain effective threshold, S_{e0}, which is located between 1800 and 2400 eV/Å in Y-Ba-Cu-O, in order to generate the deviations from the $\Delta\rho$-ΔT_{c0} scaling (Fig. 9). It might be that the precise value of S_{e0} depends on the physical property under consideration but, nevertheless, it is reasonable to assume that a considerable amount of structural alteration is induced by the electronic excitations and/or ionizations provided S_e surmounts about 2000 eV/Å. It should be noted that the existence of a threshold in S_e for damage production in Y-Ba-Cu-O has been suggested previously.[28]

The existence of such effective thresholds is long known from the research work on nuclear tracks,[29] which are caused by electronic excitations and/or ionizations of the target atoms by the passage of fast heavy ions.[29] Since, for these projectiles, the mean free path between two successive electronic excitations is of subatomic length, a continuous trail of defect forms which are (meta-) stable in track-storing materials and can be made visible by high-resolution electron microscopy. In fact, the existence of latent tracts in Y-Ba-Cu-O was evidenced by HRTEM investigations[11,13] (Fig. 10 shows a cross section of tracks observed in epitaxial Y-Ba-Cu-O films after irradiation with 173-MeV ^{129}Xe, from Ref. 13). This result definitely proves that S_e contributes to damage production in Y-Ba-Cu-O and the far-reaching conclusion of Ref. 30 is certainly not justified. It should be noted that S_{e0} does not represent a distinct electronic energy-loss threshold below which no structural modifications at all are induced by electronic excitations. Rather, due to the stochastic nature of the excitation process, S_{e0} marks the region in S_e where, with increasing S_e, the structure of Y-Ba-Cu-O becomes progressively sensitive to electronic excitations. It was found by HRTEM on ferrites,[31] that for $S_e > S_{e0}$ ion tracks are continous whereas they consist

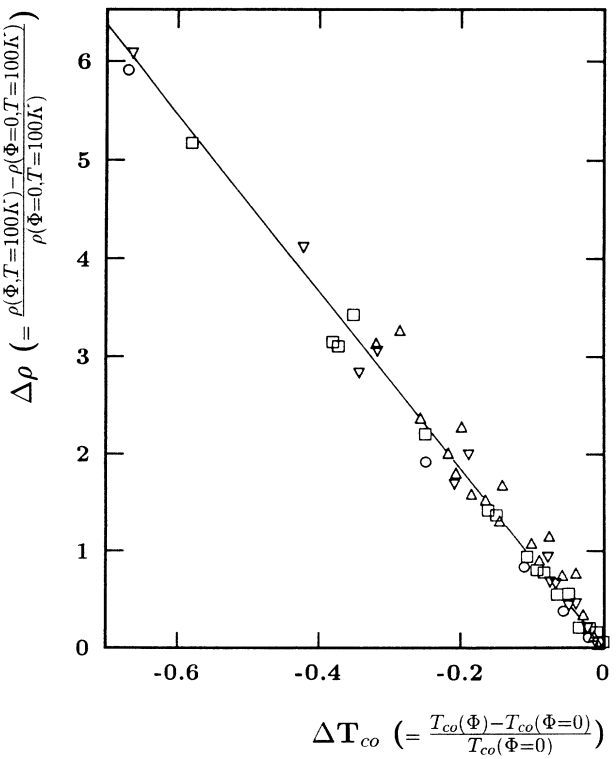

FIG. 8. $\Delta\rho$ against ΔT_{c0} for 6-MeV ^{4}He (circles), 25-MeV ^{16}O (squares), 25-MeV ^{32}S (triangles), and 120-MeV ^{86}Kr (inverted triangles).

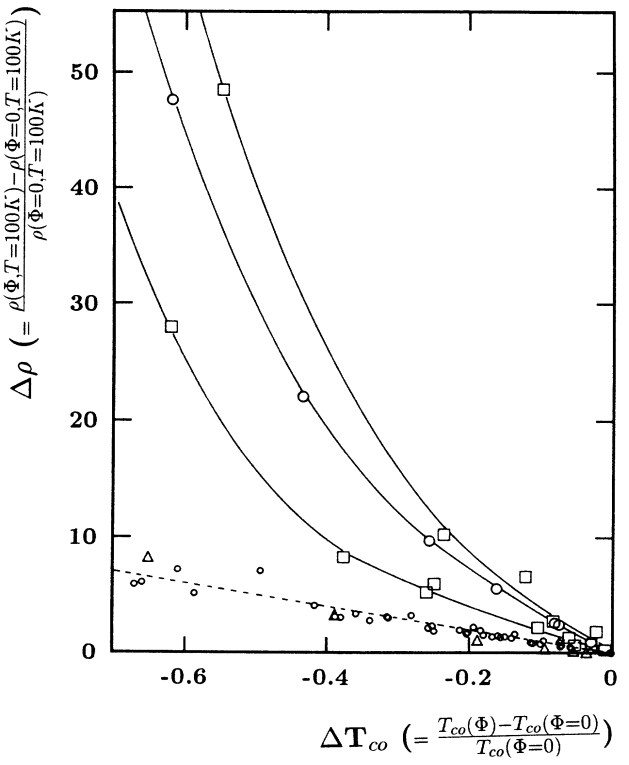

FIG. 9. $\Delta\rho$ against ΔT_{c0} for 173-MeV ^{129}Xe (circles) and 360-MeV ^{129}Xe (the two sets of squares represent the results for two different charges of samples). The results for an oxygen deficient sample ($T_{c0} \approx 60$ K before irradiation with 360-MeV ^{129}Xe) are plotted as triangles. The small circles represent the data from Fig. 8.

of strings of "pearls" of amorphized material for S_e somewhat below S_{e0}. It is suggestive to assume a similar behavior for Y-Ba-Cu-O, i.e., for 120-MeV ^{86}Kr ions and 25-MeV ^{32}S ions one can expect defect clusters lined up along the ion paths induced by S_e in addition to spatially uncorrelated defects that originate from S_n. The existence of extended latent tracks, however, was not substantiated by HRTEM studies. On the one hand, for these ions both kinds of defects should still affect the resistivity and the critical temperature in an "additive" way, explaining the linear resistivity increase with fluence observed for 120-MeV ^{86}Kr (Fig. 11). On the other hand, the S_e-induced defect strings certainly can lead to anisotropic effects on particular physical properties like, e.g., flux creep. In fact, preliminary results of $\rho(T,B)$ after irradiation substantiate this idea and they will be reported in a forthcoming publication.[21]

The experimental evidence for the existence of latent tracks of amorphized material in Y-Ba-Cu-O after irradiation with fast heavy ions ($S_e > 2000$ eV/Å) raises the question of how these tracks affect the resistivity ρ and the critical temperature T_{c0}. In the following a simple model for the anomalous irradiation behavior above the threshold S_{e0} will be proposed. The model is based on mechanical stress considerations and does not regard microscopic defects in detail.

The formation of continuous tracks of amorphized material along the ion paths surely must influence the resistivity. As amorphous Y-Ba-Cu-O is known to be a poor conductor, we would expect a resistivity increase with fluence (corresponding to the introduction of insulating cylinders into a conducting matrix) which shows "percolationlike" behavior. An apparent inconsistency of this naive assumption is the absence of a threshold for the degradation of T_{c0} with ion fluence (within experimental accuracy) that would be expected due to the existence of undisturbed paths for the supercurrent even at high fluences. Obviously there must be another mechanism that critically affects ρ and T_{c0} (this is also suggested by the different $\Delta\rho$-ΔT_{c0} correlation of Fig. 9).

The transformation of Y-Ba-Cu-O from the crystalline to the amorphous phase is accompanied by a density deficit, i.e., the density of the amorphous material is slightly lower than of the perfect crystal. This deficit, in turn, must result in a volume increase, as no material vanishes. This expansion, however, is hindered by the surrounding matrix (except at the faces of the cylinders) and so stresses will develop near the tracks. Such stress fields have been postulated in Ref. 31 to surround a highly distorted second shell around an amorphous core of latent tracks in $Y_3Fe_5O_{12}$. These highly anisotropic stresses (major axis in the *ab* planes) are connected with strains of the *a* and *b* axes, and also of the *c* axis. From x-ray-diffraction patterns[13] an elongation of the *c* axis is calculated to $e_{zz}=2.5\%$ at a fluence of 3.5×10^{12}cm^{-2} 173-MeV ^{129}Xe. This extension of the *c* axis by far exceeds the values obtained for samples of the same reduced T_{c0} that were irradiated with 25-MeV ^{16}O, where

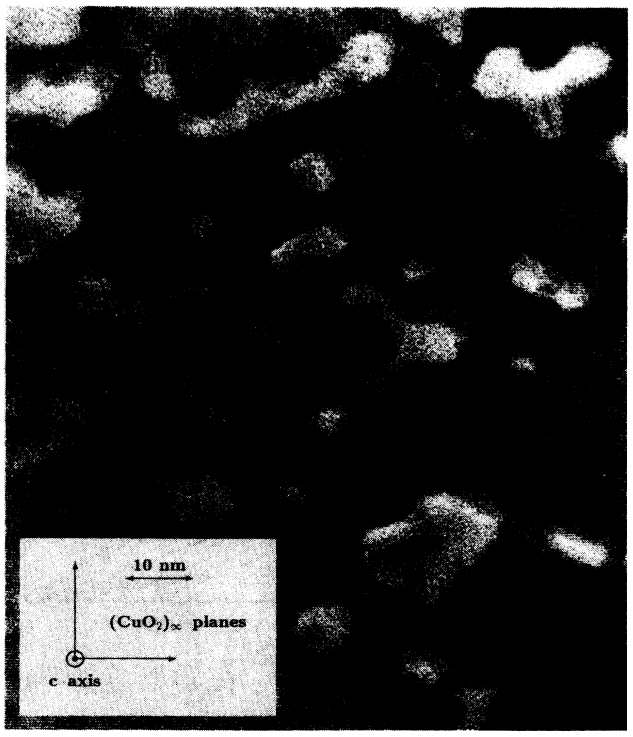

FIG. 10. HRTEM image of the tracks of 173-MeV ^{129}Xe in epitaxial Y-Ba-Cu-O films in "plane view" ($\Phi=2\times10^{12}$ cm^{-2}). The incident direction of the ions was perpendicular to the film plane (picture from Ref. 13).

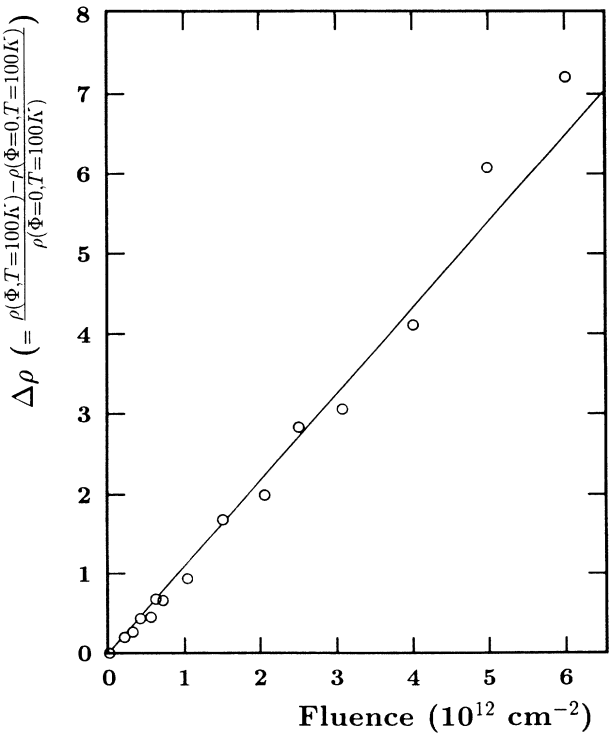

FIG. 11. $\Delta\rho$ vs fluence for 120-MeV ^{86}Kr.

only a small elongation is observed. Even the values of samples with comparable T_{c0} prepared with oxygen deficiency[32] are significantly smaller. In Ref. 13 we have outlined a simple geometrical model that enables us to describe quantitatively this elongation of the c axis with fluence. It should be noted that the x-ray-diffraction patterns have been recorded at room temperature after annealing the samples for several days.

From experiments[33] which investigated the influence of uniaxial c-axis stress on ρ_c and T_c^{onset} of Y-Ba-Cu-O single crystals, a strong dependence of these parameters on the interplane coupling of the Cu-O layers is evident. The value of the T_c^{onset} increase ($dT_c^{\text{onset}}/dp \approx 0.8$ K/GPa) agrees well with data obtained from measurements performed on polycrystalline samples under hydrostatic pressure.[34] By assuming a decrease of T_c^{onset} for an elongation of the c axis, it is possible to estimate the T_c^{onset} decrease from the strain of the c axis. With the elastic constants taken from Ref. 35 ($C_{33}=185$ GPa) we calculate the c-axis stress to approximately $\sigma_{zz}=C_{33}e_{zz}=5$ GPa for a strain of 2.5% and thus a T_c^{onset} reduction of about 4 K would be expected. At first sight this value is too small to fit our data, but Fig. 1(b) reveals that for ^{129}Xe the onset to superconductivity is much less affected by irradiation than the completion of the transition T_{c0} which we discussed so far. In fact, a shift of T_c^{onset} by less than 10 K can be seen from Fig. 1(b) for a fluence of 3×10^{12} cm^{-2} 360-MeV ^{129}Xe. Furthermore, we observe very strong annealing effects (about 50% of the T_{c0} decrease and the resistivity increase are recovered after annealing the samples for 1 h at 300 K) which are not observed for the light projectiles 6-MeV ^{4}He and 25-MeV ^{16}O. It is suggestive to assume that these strong effects originate from the relaxation of stress due to the thermal treatment.

The "stress model" allows a discussion of the broadening of the phase transitions at higher fluences. The randomly distributed track positions will result in very different strains spread over the sample and so it is plausible that a wide distribution of T_{c0} will exist. The sample areas with the smallest strain (i.e., the highest T_c) determine T_c^{onset} (this is the "unaffected matrix" of Fig. 10), while the superconducting path required for T_{c0} certainly must pass regions of considerably higher strains (i.e., low T_c) and, in the worst case, no such path is present, resulting in extremely broadened transitions that are, in fact, observed experimentally [Fig. 1(b)].

It should be noted that the deviations from the scaling behavior are extremely sensitive to sample quality. Samples of inferior quality (e.g., poorer oxygen content) do not exhibit any deviations (Fig. 9, triangles), while the strongest effects are observed for the "best samples" (high T_{c0}, narrow transition, low resistivity). If "high quality" is connected with the perfection of the crystal lattice, this observation can be explained by the assumption that stresses can be released at grain or twin boundaries by plastic deformations. The defects of such distorted regions will significantly affect T_{c0} while the macroscopically averaged resistivity will be less influenced. This leads to a $\Delta\rho$-ΔT_{c0} correlation similar to those observed for the light projectiles. To conclude we want to underline that the "stress model" enables us to interpret most of the observed effects satisfactorily with only few reasonable assumptions, despite the very crude approximations that are made and the lack of reliable data for the "input parameters" of the model.

ACKNOWLEDGMENTS

The authors would like to thank all members of the low-temperature physics group of the Physikalisches Institut Erlangen for assistance in the experiments and helpful discussions. One author (B.H.) would like to thank L. Schultz and H.E. Hoenig of Siemens AG, Erlangen, for making available the samples. Financial support by the Bundesminister für Forschung und Technologie is gratefully acknowledged.

*Also at Siemens AG, Erlangen, Federal Republic of Germany.

[1]G. J. Clark, A. D. Marwick, F. Legoues, R. B. Laibowitz, R. Koch, and P. Madakson, Nucl. Instrum. Methods B **32**, 405 (1988).

[2]A. E. White, K. T. Short, D. C. Jacobson, J. M. Poate, R. C. Dynes, P. M. Mankiewich, W. J. Skocpol, R. E. Howard, M. Anzlowar, K. W. Baldwin, A. F. J. Levi, J. R. Kwo, T. Hsieh, and M. Hong, Phys. Rev. B **37**, 3755 (1988).

[3]G. C. Xiong, H. C. Li, G. Linker, and O. Meyer, Phys. Rev. B **38**, 240 (1988).

[4]A. Iwase, N. Masaki, T. Iwata, T. Nihira, and S. Sasaki, Jpn. J. Appl. Phys. **27**, L2071 (1988).

[5]J. O. Willis, D. W. Cooke, R. D. Brown, J. R. Cost, J. F. Smith, J. L. Smith, R. M. Aikin, and M. Maez, Appl. Phys. Lett. **53**, 417 (1988).

[6]A. E. White, K. T. Short, R. C. Dynes, A. F. J. Levi, M. Anzlowar, K. W. Baldwin, P. A. Polakos, T. A. Fulton, and L. N. Dunkleberger, Appl. Phys. Lett. **53**, 1010 (1988).

[7]B. Roas, B. Hensel, G. Saemann-Ishenko, and L. Schultz, Appl. Phys. Lett. **54**, 1051 (1989).

[8]J. M. Valles, Jr., A. E. White, K. T. Short, R. C. Dynes, J. P. Garno, A. F. J. Levi, M. Anzlowar, and K. Baldwin, Phys. Rev. B **39**, 11 599 (1989).

[9]O. Meyer, B. Egner, G. C. Xiong, X. X. Xi, G. Linker, and J. Geerk, Nucl. Instrum. Methods B **39**, 628 (1989).

[10]D. Bourgault, S. Bouffard, M. Toulemonde, D. Groult, J. Provost, F. Studer, N. Nguyen, and B. Raveau, Phys. Rev. B **39**, 6549 (1989).

[11]D. Bourgault, M. Hervieu, S. Bouffard, D. Groult, and B. Raveau, Nucl. Instrum. Methods B **42**, 61 (1989).

[12]A. D. Marwick, G. J. Clark, D. S. Yee, R. B. Laibowitz, G. Coleman, and J. J. Cuomo, Phys. Rev. B **39**, 9061 (1989).

[13]B. Roas, B. Hensel, S. Henke, S. Klaumünzer, B. Kabius, W. Watanabe, G. Saemann-Ischenko, L. Schultz, and K. Urban, Europhys. Lett. **11**, 669 (1990).

[14]S. Klaumünzer, C. Li, S. Löffler, M. Rammensee, and G. Schuhmacher, Nucl. Instrum. Methods B **39**, 665 (1989).

[15]F. Studer, C. Houpert, D. Groult, and M. Toulemonde, Radiat. Eff. **110**, 55 (1989).

[16]G. Fuchs, F. Studer, E. Balanzat, D. Groult, M. Toulemonde,

and J. C. Jousset, Europhys. Lett. **3**, 321 (1987).
[17]A. Audouard, E. Balanzat, G. Fuchs, J. C. Jousset, D. Lesueur, and L. Thome, Europhys. Lett. **3**, 327 (1987).
[18]E. Paumier, M. Toulemonde, J. Dural, F. Rullier-Albenque, J. P. Girard, and P. Bogdanski, Europhys. Lett. **10**, 555 (1989).
[19]A. Dunlop, D. Lesueur, J. Morillo, J. Dural, R. Spohr, and J. Vetter, Nucl. Instrum. Methods B **48**, 419 (1990).
[20]B. Roas, L. Schultz, and G. Endres, Appl. Phys. Lett. **53**, 1557 (1988).
[21]B. Hensel (unpublished).
[22]B. Roas, G. Saemann-Ischenko, and L. Schultz, Phys. Rev. Lett. **64**, 479 (1990).
[23]J. Schützmann, W. Ose, J. Keller, K. F. Renk, B. Roas, L. Schultz, and G. Saemann-Ischenko, Europhys. Lett. **8**, 679 (1989).
[24]N. Klein, G. Müller, H. Piel, B. Roas, L. Schultz, U. Klein, and M. Peiniger, Appl. Phys. Lett. **54**, 757 (1989).
[25]A. A. Valenzuela, B. Daalmans, and B. Roas, Electron. Lett. **25**, 1435 (1989).
[26]J. Dengler, G. Ritter, G. Saemann-Ischenko, B. Roas, L. Schultz, B. Molnar, D. L. Nagy, and I. S. Szücs, Physica C **162-164**, 1297 (1989).
[27]J. P. Biersack and L. G. Haggmark, Nucl. Instrum. Methods **174**, 257 (1980).
[28]E. Balanzat, Radiat. Eff. **110**, 99 (1989).
[29]R. L. Fleischer, P. B. Price, and R. M. Walker, *Nuclear Tracks in Solids* (California Press, Berkeley, 1975).
[30]G. P. Summers, E. A. Burke, D. B. Chrisey, M. Nastasi, and J. R. Tesmer, Appl. Phys. Lett. **55**, 1469 (1989).
[31]C. Houpert, M. Hervieu, D. Groult, F. Studer, and M. Toulemonde, Nucl. Instrum. Methods B **32**, 393 (1988).
[32]B. Roas, B. Hensel, G. Endres, L. Schultz, S. Klaumünzer, and G. Saemann-Ischenko, Physica C **162-164**, 135 (1989).
[33]M. F. Crommie, Amy Y. Liu, A. Zettl, Marvin L. Cohen, P. Parilla, M. F. Hundley, W. N. Creager, S. Hoen, and M. S. Sherwin, Phys. Rev. B **39**, 4231 (1989).
[34]A. Driessen, R. Griessen, N. Koeman, E. Salomons, R. Brouwer, D. G. de Groot, K. Heeck, H. Hemmes, and J. Rector, Phys. Rev. B **36**, 5602 (1987).
[35]R. C. Baetzold, Phys. Rev. B **38**, 11 304 (1988).

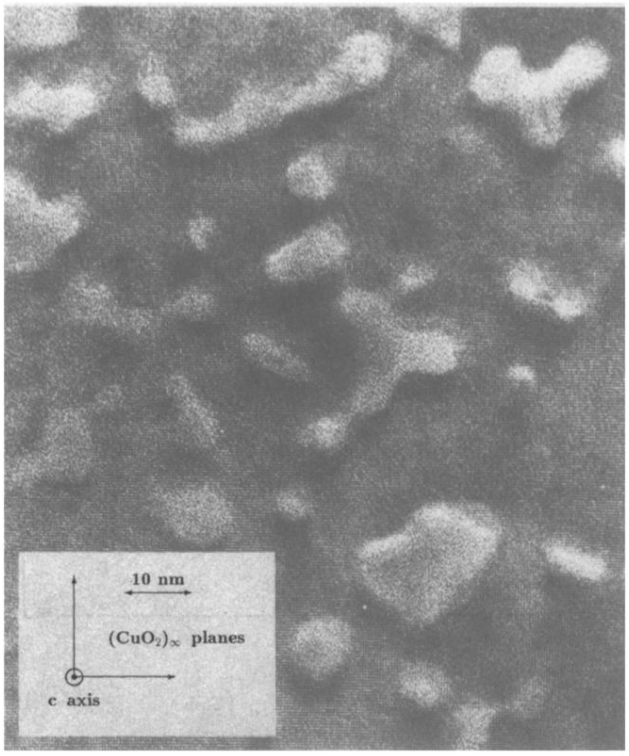

FIG. 10. HRTEM image of the tracks of 173-MeV ^{129}Xe in epitaxial Y-Ba-Cu-O films in "plane view" ($\Phi = 2 \times 10^{12}$ cm^{-2}). The incident direction of the ions was perpendicular to the film plane (picture from Ref. 13).